



HAL
open science

Two-step synthesis of VO₂(M) tuned crystallinity

Shian Guan, Aline Rougier, Oudomsack Viraphong, Dominique Denux,
Nicolas Penin, Manuel Gaudon

► **To cite this version:**

Shian Guan, Aline Rougier, Oudomsack Viraphong, Dominique Denux, Nicolas Penin, et al.. Two-step synthesis of VO₂(M) tuned crystallinity. *Inorganic Chemistry*, 2018, 57 (15), pp.8857-8865. 10.1021/acs.inorgchem.8b00753 . hal-01871116

HAL Id: hal-01871116

<https://hal.science/hal-01871116>

Submitted on 23 Nov 2023

HAL is a multi-disciplinary open access archive for the deposit and dissemination of scientific research documents, whether they are published or not. The documents may come from teaching and research institutions in France or abroad, or from public or private research centers.

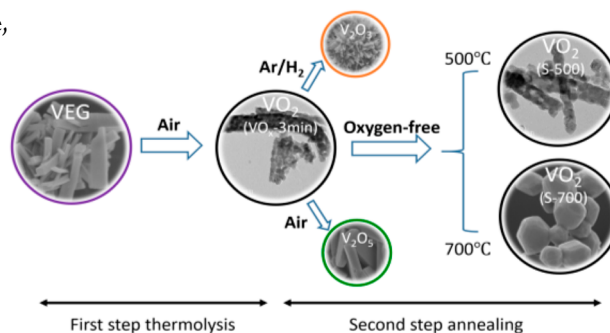
L'archive ouverte pluridisciplinaire **HAL**, est destinée au dépôt et à la diffusion de documents scientifiques de niveau recherche, publiés ou non, émanant des établissements d'enseignement et de recherche français ou étrangers, des laboratoires publics ou privés.

Two-Step Synthesis of VO₂ (M) with Tuned Crystallinity

Shian Guan, Aline Rougier, Oudomsack Viraphong, Dominique Denux, Nicolas Penin, and Manuel Gaudon*

CNRS, Université de Bordeaux, ICMCB UMR 5026, Pessac, F-33600, France

ABSTRACT: Highly crystallized monoclinic vanadium dioxide, VO₂ (M), is successfully synthesized by a two-step thermal treatment: thermolysis of vanadyl ethylene glycolate (VEG) and postannealing of the poorly crystallized VO₂ powder. In the first thermolysis step, the decomposition of VEG at 300 °C is investigated by X-ray diffraction and scanning electron microscopy (SEM). A poorly crystallized VO₂ powder is obtained at a strict time of 3 min, and it is found that the residual carbon content in the powder played a critical role in the post crystallization of VO₂ (M). After postannealing at 500 and 700 °C in an oxygen-free atmosphere, VO₂ particles of various morphologies, of which the crystallite size increases with increasing temperature, are observed by SEM and transmission electron microscopy. The weight percent of crystalline VO₂, calculated using the Fullprof program, increases from 44% to 79% and 100% after postannealing. The improved crystallinity leads to an improvement in metal–insulator transition behaviors demonstrated by sharper and more intense differential scanning calorimetry peaks. Moreover, V₂O₃ and V₂O₅ with novel and particular microstructures are also successfully prepared with a similar two-step method using postannealing treatment under reductive or oxidizing atmospheres, respectively.



1. INTRODUCTION

More than 10 kinds of vanadium dioxide (VO₂) crystalline phases have been reported in the literature. Tremendous research efforts have been devoted to the various VO₂ polymorphs syntheses.^{1–11} At low temperature, monoclinic VO₂ (M) is the most stable one and undergoes a first-order metal–insulator transition (MIT) to rutile phase VO₂ (R) at 68 °C associated with a drastic change in optical properties in the near-infrared range.^{4,6} Owing to these properties, VO₂ (M) has been considered in a wide range of applications including optical switching, optical sensing, and in particular as a strong candidate for smart windows because of its significant effect in energy savings.^{4,12–15} Indeed, windows are known as one of the most energy-inefficient components of buildings. VO₂-based thermochromic smart windows exhibit a self-regulating ability of optical transmission/reflection with temperature changes near room temperature, and so, they offer smart functions to decrease building energy consumption.

In close relation with smart window applications, the VO₂ (M) phase is mainly directly elaborated as thin films on glass substrates by physical deposition processes as magnetron sputtering, pulsed laser deposition (PLD), or epitaxial growth.¹⁶ More recently, several methods have been reported to prepare VO₂ nanoparticles, such as the sol–gel synthesis,¹⁷ hydrothermal synthesis,^{2,18} and pyrolysis method.^{17,19} In comparison with physical deposition processes, the use of nanoparticles presents some advantages in energy efficiency owing to their small size, large surface area, great chemical reactivity, and mechanical strength associated with a low cost

coating process at room temperature and at atmospheric pressure. The processes based on the pyrolysis of a vanadium oxide precursor have gained popularity,^{17,19} since (i) the VO₂ (M) composition (the homogeneous doping with various metallic elements is shown and the V/O ratio can be tuned) can be controlled from the parameters of the pyrolysis step (oxygen partial pressure, temperature), (ii) this synthesis route is really easy to set up (in comparison to hydrothermal processes, for illustration), and (iii) it shows a prospect of mass production. As a commonly used vanadium precursor, vanadyl ethylene glycolate (VEG) has been investigated through the pyrolysis method to synthesize VO₂ (M) submicronic powder.^{20,21} In our group, Mjejri et al. reported the synthesis of VO₂ powder from a single polyol route by annealing the VEG directly under very low oxygen pressure ($\sim 10^{-5}$ Pa).²¹ In order to eliminate or weaken the effect of energy surplus during VEG decomposition, Zhang et al. prepared VO₂ by dividing the VEG pyrolysis process into two steps.²² Zou et al. obtained VO₂ powder via the thermolysis of VEG precursor in air atmosphere.²³ However, most of the studies in the literature focused on the thermochromic properties of synthesized VO₂ powders, while the study of the decomposition of VEG with different annealing temperatures has not yet been investigated. Moreover, the versatility of the oxidation number of vanadium leads to the difficulty to propose a robust flow-chart for a reproducible synthesis. Furthermore, even if all the studies

point out the need for high crystalline quality for VO₂ powder, as far as we know, this aspect was not deeply investigated in previous studies by following the crystalline fraction from accurate X-ray investigations. This is a key issue as the occurrence of undesired amorphous VO₂ without any thermochromic properties would act drastically to the detriment of the smart optical/electrical effect of the as-prepared powders. Thus, the calculation of VO₂ (M) crystallinity appears necessary and could greatly help us to evaluate the particles' thermochromic performances.

Herein, pure VO₂ (M) powder with high crystallinity is synthesized through a two-step thermolysis and postannealing process. The VEG is first decomposed in air, and a poorly crystallized VO₂ powder is obtained after 3 min heating, prior to further annealing at higher temperatures in an oxygen-free environment for a full-crystallization. The crystallinity of three different VO₂ powders is carefully determined in parallel with the VO₂ particles morphological evolution. The VEG decomposition in the first step is investigated carefully, and it is found the carbon plays an important role in the second step of VO₂ crystallization. Moreover, novel and particular microstructures for V₂O₃ and V₂O₅ compounds are also synthesized through this method changing the atmosphere of the second step annealing.

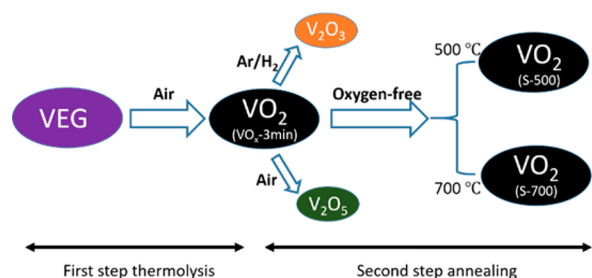
2. EXPERIMENTAL SECTION

2.1. Materials. Ammonium metavanadate (NH₄VO₃; 99.0%) was purchased from PROLABO. Ethylene glycol (C₂H₆O₂) was purchased from Sigma. Aldrich, Co. All the chemicals reagents were used as obtained commercially without further purification.

2.2. Synthesis. **2.2.1. First Step Thermolysis for the VEG Decomposition.** A total of 1.42 g of NH₄VO₃ powder was mixed with a certain amount of C₂H₆O₂ in a 250 mL three-neck flask and heated to 160 °C under vigorous stirring as reported.²¹ The precipitate was collected by centrifugation, washed with ethanol three times, and dried overnight in oven at 80 °C to remove excess of ethanol. Then the obtained vanadyl ethylene glycolate (VEG) precursor was heated in the furnace (air) at 300 °C for durations from 1 to 90 min.

2.2.2. Post Annealing Treatment of Poorly Crystallized VO₂ Powder. The resulting powders from first step were further annealed in a nearly oxygen-free atmosphere (PO₂ < 10⁻⁴ bar) to enhance their crystallinity of VO₂ powders. After the decomposition of VEG for 3 min at 300 °C, the powder (VO_x-3 min) was chosen as the starting material for the post annealing for 5 h at temperatures of 500 and 700 °C in the second step, as illustrated by Scheme 1. The annealing temperature was controlled by a temperature controller with a heating rate of about 10 °C/min. Furthermore, V₂O₃ and V₂O₅ with new and particular morphologies were prepared by annealing VO_x-3 min powder under different conditions: 800 °C for 0.5 h under Ar/H₂ atmosphere (95:5 mol % ratio) for the preparation of vanadium

Scheme 1. Illustrations of the Preparation of VO₂, V₂O₃, and V₂O₅



sesquioxide, and 600 °C for 0.5 h under air for the preparation of vanadium pentoxide.

2.3. Characterizations. The crystal structures of the as-prepared samples were determined by X-ray diffraction (XRD) analyses (Philips PW1820, PANalytical X' Pert PRO MPD diffractometer) performed using a Cu-K α 1 radiation source ($\lambda = 1.54056 \text{ \AA}$), with a divergent slit of 1° and receiving slit size of 0.1 mm in a 2θ range from 8° to 80°. The identification of compounds was made by comparing the experimental XRD patterns to standards compiled by the Joint Committee on Powder Diffraction and Standards. Moreover, Rietveld refinements were performed using FullProf software. The morphology of the as-prepared particles was observed by SEM using a TESCAN Vega II SBH microscope and JEOL JSM-6700F, and also by high resolution transmission electron microscopy (HRTEM, JEOL 2200FS, operating at 200 kV). Carbon content of each sample was determined by CHNS elementary analyzer (Thermo Fisher Scientific). Thermogravimetric analysis (TGA) was carried out on a Setaram TGA instrument. Differential scanning calorimetry (DSC) experiment of as-obtained VO₂ powders was performed using PerkinElmer DSC. The reflectance spectra were measured using a Varian Cary UV-vis-NIR spectrophotometer in a wavelength region from 200 to 2500 nm.

3. RESULTS AND DISCUSSION

3.1. Decomposition of VEG. Vanadyl ethylene glycolate (VEG: VC₂H₄O₃) is prepared by polyol synthesis to be used as vanadium precursor. During its preparation, V(V) in NH₄VO₃ is reduced to V(IV) by ethylene glycol (EG) with the consequent formation of vanadyl complex. EG is not only a well-known solvent used in the polyol method to prepare highly divided metal particles, but also a cross-linking reagent coordinating to the central metal ion to form a metal glycolate further leading to subsequent oligomerization.

To fully decompose VEG in a short time, referring to our own TGA measurements as well as the one reported with DSC data by Zhang et al.,²² the VEG is annealed in air at 300 °C for various times (1–5 min, 8 and 90 min). As shown in Figure 1, VEG gradually transforms into VO₂ and then V₂O₅ after air annealing. During the pyrolysis process of VEG, the effect of the annealing treatment can be separated into two stages.

In the first stage (0–3 min), the VEG precursor starts to decompose and forms a poorly crystallized VO₂ phase, consecutively to carbon chain combustion, as described in eq 1.

The intensity of the peak located at $2\theta = 13.46^\circ$ corresponding to a preferred (110) Miller orientation of the VEG compound decreases gradually during heating at 300 °C in the first 2 min with simultaneous rising of VO₂ (M) peaks (the main peak being located at $2\theta = 27.95^\circ$).

Two phases VO₂ (M) as a major phase and VO₂ (B) as a minor one coexist after the heating treatment for 3 min, named VO_x-3 min, while no more VEG peaks are detected. With continuous heating, V(V) containing phases start to emerge due to the further oxidation in the second stage (4–90 min), as shown in eq 2.

XRD results show that traces of vanadium(V) oxide powders (V₂O₅ and V₆O₁₃) start to form at 4–5 min, resulting from the partial energy surplus due to the exothermic process of VEG decomposition.²² After 8 min annealing, some new peaks (like $2\theta = 20.26^\circ$ and 26.26°) (Figure 1), which belong to V₂O₅ (space group: *Pmnn*, JCPDS No. 41-1426), appear, and VO₂ coexists with V₂O₅. Finally, VO₂ is entirely converted to V₂O₅ after VEG being heated for 90 min.

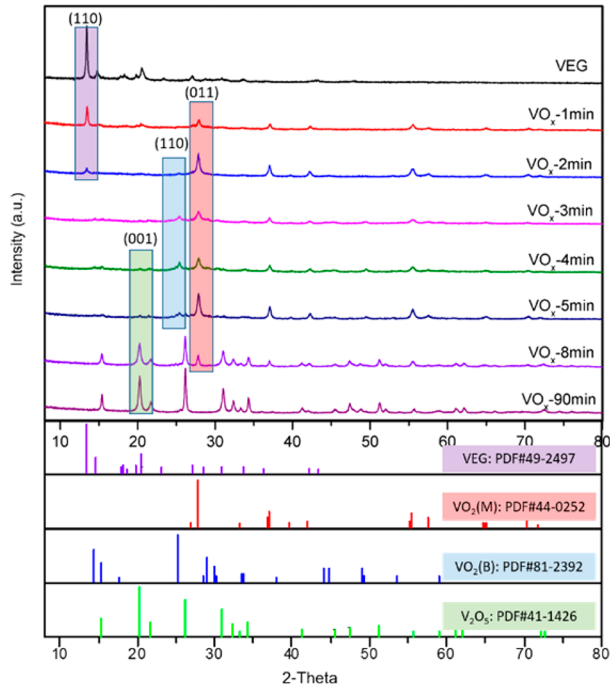


Figure 1. XRD patterns of samples synthesized by thermolysis of VEG precursor at 300 °C in air with different annealing times (1–5 min, 8 and 90 min). Corresponding PDF numbers provided at the bottom.

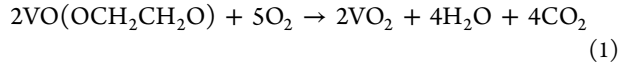


Figure 2a insets displays the photos of the VO_x obtained powders after decomposition of the VEG precursor. For

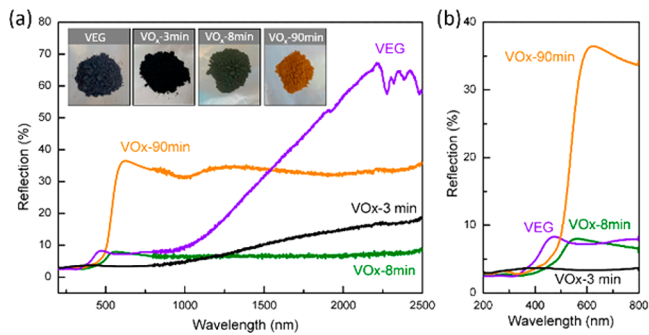


Figure 2. (a) The reflection spectra of the VEG, VO_x -3 min, VO_x -8 min, and VO_x -90 min samples in the wavelength region of 200–2500 nm; insets show photos of the VEG and VO_x samples; and (b) their reflection spectra in the visible region of 200–800 nm.

deeper comparison of the optical properties of the decomposition products, the reflection spectra measured in the 200–2500 nm and in the UV–visible region (200–800 nm) are shown in Figure 2b, respectively. Undecomposed VEG shows a bluish gray color, corresponding to a reflection of visible radiation at around 470 nm. The color changes to black after being heated for 3 min with a rather flat reflectance spectra of less than 5% in the visible region, corresponding to the color of VO_2 powder. After longer heating, an orange color starts to emerge due to the presence of the V_2O_5 phase. At 8 min, the

orange mixes with the remaining black color from VO_2 , and the color of the obtained powder becomes dark green (VO_x -8 min), and the reflection gap shifts to a higher wavelength (i.e., 560 nm). Finally, a full orange color appears after 90 min, which indicates the complete oxidation in V_2O_5 , with a clear charge transfer band gap located at about 600 nm. The color of each powder is consistent with the evolution of the phases previously detected by XRD data in Figure 1.

The corresponding morphologies from low-magnification SEM (Figure 3) consist of elongated cuboids that remain

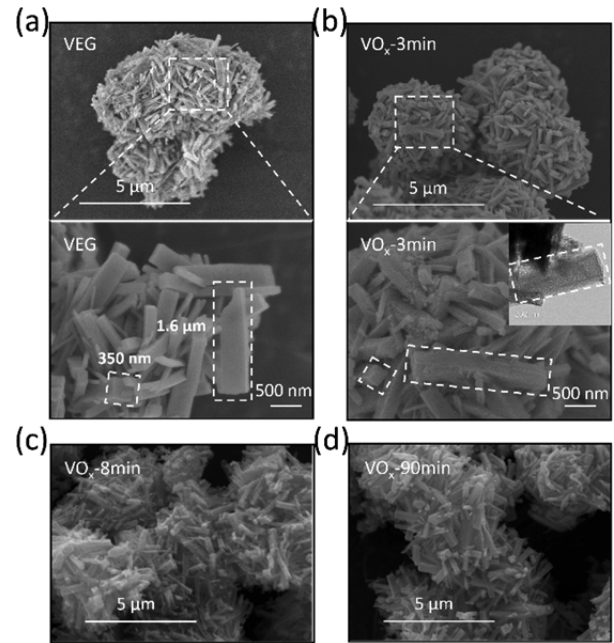


Figure 3. SEM images of (a) VEG, and its decomposed products at 300 °C for different times: (b) VO_x -3 min (inset shows the evident porosity from its corresponding TEM), (c) VO_x -8 min, and (d) VO_x -90 min.

basically unchanged after heating at 300 °C for 90 min. Because of the large surface energy, these cuboids easily aggregate, forming spherical aggregates about 5 μm in size.

In order to gain further insight into the decomposition process of VEG, VEG, and VO_x -3 min samples were characterized by high resolution SEM. As shown in Figure 3a, VEG nanostructures exhibit an elongated cuboid morphology and a typical length of several micrometers ($\sim 1.6 \mu\text{m}$) and an average length of $\sim 350 \text{ nm}$ (in its rectangular cross section). After 3 min heating in air and removal of the organic components (C and H), the cuboid shape remains, while the detailed morphology as cuboid surface changes from smooth to rough aspect (Figure 3a,b). Combined with its TEM image (inset in Figure 3b), the structure of cuboid after decomposition could be seen more clearly and composed of numerous small particles, which can be attributed to the removal of the organic part in the form of CO_2 and H_2O during the VEG annealing (eq 1); i.e., the small particles can be attributed to the appearance of the VO_2 crystallites. Hence, VEG crystallites are shown to be the “reservoirs” of the germination and growth of the VO_2 phase. The morphology of the nanometric VO_2 issued from VEG decomposition is so “templated” by the VEG crystallite shape. A powder architecture at two different scales is observed:

isotropic VO₂ crystallites with growing size versus calcination duration are aggregated in a way that the polycrystalline assemblies retain the initial VEG crystallite shape and size.

3.2. Postannealing Treatment of VO_x-3 min. **3.2.1. Synthesis of VO₂.** From the combination of the XRD data and morphology of decomposed products, the optimal time of heating VEG is around 3 min. The VO₂ powder (VO_x-3 min) obtained from VEG decomposition is of relatively poor crystallinity due to the short heating time (3 min) at a rather low temperature (300 °C), as confirmed by the wide XRD peaks (Figure 1).

Thus, a postannealing treatment at higher temperature for the VO_x-3 min sample is necessary to prepare VO₂ powder with a higher crystallinity. During the second annealing step, it was found that the decomposition time for the VEG in the first step plays a critical role in the formation of VO₂.

Four samples with different decomposition times in the first step (VEG, VO_x-2 min, VO_x-3 min, and VO_x-5 min) were chosen for a higher temperature postannealing treatment. These samples were heat treated at 500 °C for 5 h in an environment free of oxygen (PO₂ < 10⁻⁴ bar) in order to avoid VO₂ from being oxidized into V₂O₅.

As organic components, carbon materials are usually used as a reducing agent, like hydrazine reported by Cao et al.,⁵ and thus the carbon content of each sample is measured through CHNS before annealing, and its evolution vs heating time is shown in Figure 4a. Overall, the carbon content decreases

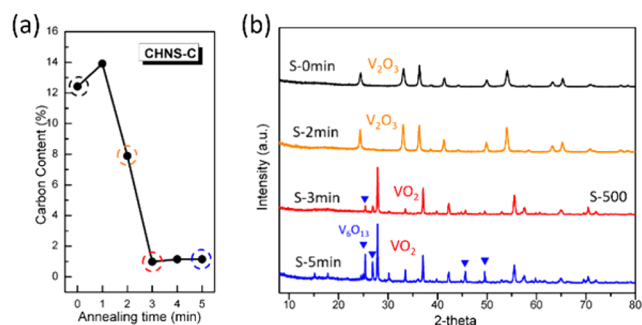


Figure 4. (a) Carbon content of samples obtained through heating VEG with different times at 300 °C in air (1–5 min). (b) The XRD patterns of samples (S-0 min, S-2 min, S-3 min, and S-5 min) synthesized after a postannealing treatment at 500 °C for 5 h in an oxygen-free atmosphere from VEG, VO_x-2 min, VO_x-3 min, and VO_x-5 min, respectively (S-3 min was further named S-500).

during the decomposition (eq 1). The initial VEG contains 12.42% of carbon. After a decomposition time of 2 min, 7.89% of carbon still exists in the VO_x-2 min sample, which can be attributed to undecomposed VEG remaining in the powder. After VEG is heated for 3 min (VO_x-3 min), the carbon content decreases to 0.98%, indicating the nearly full decomposition of VEG. The residual carbon content remains unchanged for longer annealing times (VO_x-4 min and VO_x-5 min). The carbon contents of most samples before and after annealing at 500 °C are gathered in Table S1 in the Supporting Information.

The XRD patterns of postannealing samples are shown in Figure 4b. The 500 °C postannealing of VO_x-3 min leads to the so-called S-3 min sample. Pure V₂O₅ (S-0 min) is obtained when VEG is annealed at 500 °C in an oxygen-free atmosphere, in agreement with previously reports showing that only V₂O₅ can be obtained under inert atmospheres.^{22,23}

Unexpectedly, the XRD of S-2 min sample also shows a pure V₂O₅ phase (Figure S1). The lack of VO₂ peaks after post annealing treatment indicates that the V(IV) is probably reduced to V(III) by reducing agents for the VO_x-2 min sample that is in fact a combination of VEG and VO₂ (Figure 1) and that contains quite a lot of carbon (7.89%). The existence of carbon probably causes the reduction of VO₂ to V₂O₃. When the VEG is heated for longer times (3 and 5 min), the carbon content further decreases to a quite low level (0.98%) (Figure 4a), which might avoid the reduction from VO₂ to V₂O₃. The XRD pattern of the S-3 min and the S-5 min samples showing mainly VO₂ (M) phase (Figure 4b) confirms our hypothesis that there is no V(III) after the postannealing treatment. However, in the S-3 min sample especially in the S-5 min sample, peaks of undesired V₆O₁₃ phase, known as a V(IV) and V(V) mixed valence oxide,^{20,30} are visible. Its presence probably results from excessive oxidation during the VEG decomposition in the first step (Figure 1 and eq 2).

To summarize, a relatively pure VO₂ phase (S-3 min, called later S-500) with high crystallinity is synthesized by our two-step thermal process. First, a thermolysis step allows the preparation of poorly crystallized VO₂ (VO_x-3 min), by decomposing the VEG in a strict heating time (~3 min). The organic part of undecomposed VEG remaining in the powder when the heating time is shorter than 3 min will contribute to reduce the VO₂ to V₂O₃ in the follow-up postannealing treatment. On the contrary, V(V) coexists with V(IV) in the powder when the decomposition process is longer than 3 min.

As V(V) is the most stable vanadium state,³⁰ it is difficult to remove once it is formed. Those results emphasize that the decomposition time for VEG in the first thermolysis needs to be controlled very accurately.

To study the influences of crystallized temperature on VO₂ powders,²⁴ VO_x-3 min sample is chosen as the starting material for the postannealing treatment at a higher temperature (700 °C) in an oxygen-free environment (S-700). In an attempt to clarify structural analysis, XRD data were processed by the software program Fullprof, and the Rietveld structure refinement is shown in Figure 5a and Table 1. With satisfactory convergence factors ($R_{\text{Bragg}} = 4.85$, $R_f = 4.2$), the diffraction pattern is refined as the monoclinic phase of VO₂ (M) (space group $P2_1/c$), with lattice parameters $a = 5.7550(1)$ Å, $b = 4.5291(7)$ Å, $c = 5.3854(8)$ Å, and $\beta = 122.6030(4)^\circ$. The corresponding structure deduced from unit cell parameters and V, O atomic positions extracted from Rietveld refinement is shown in Figure 5b. We confirm that the structure and atomic positions match with JCPDS data card 00-044-0252 from the reported structure of monoclinic VO₂.¹⁴ No characteristic peaks of any other phases are detected, indicating that the sample is highly pure. Traces of V₂O₅ and V₆O₁₃, which were detected in the VO_x-3 min powder before postannealing, are probably reduced to VO₂ during annealing at high temperature.³¹ This reduction is helped by a mechanism of dilution of the minor phases into the VO₂ main phase in order to decrease the surface energies (cosintering phenomenon).

The morphologies of VO₂ powders synthesized by VEG decomposition (VO_x-3 min), and postannealing of VO_x-3 min sample at 500 °C (S-500) and 700 °C (S-700) for 5 h, are displayed in Figure 6. The VO_x-3 min sample shows a cuboid structure composed of uniform nanoparticles (Figure 6a). After postannealing at 500 °C, the elongated shape of the cuboids of VO₂ starts to break down and becomes a rod-like structure (Figure 6b) composed of larger nanoparticles. When

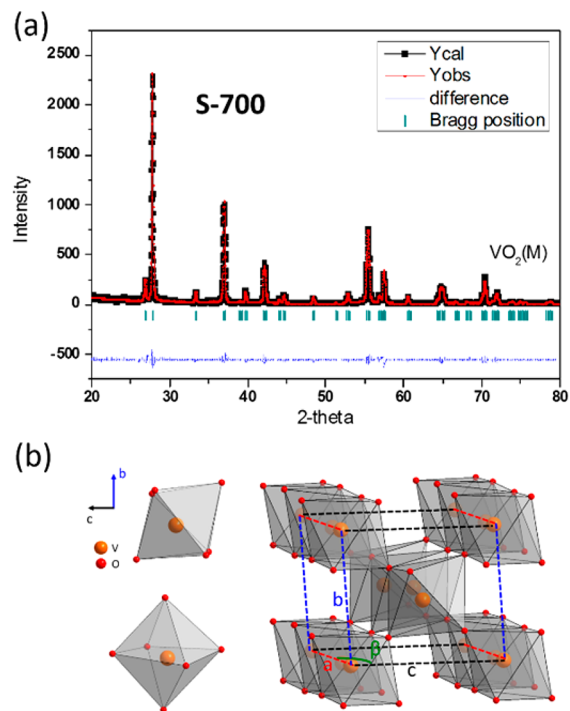


Figure 5. (a) Rietveld refinement of X-ray diffraction pattern for VO_2 (M) (S-700) synthesized at 700°C for 5 h through post annealing of VO_x -3 min powder. The observed and calculated intensities are represented by red cross and black solid line, respectively. The bottom blue line shows the fitting residual difference. The Bragg positions are represented by dark cyan ticks. (b) The refined structure of monoclinic VO_2 (M). The octahedron unit consists of one vanadium atom and six oxygen atoms, which are colored orange and red, respectively.

the postannealing temperature is increased to 700°C , the rod-like structure is further broken down, and the isolated VO_2 particles become more regular with clear grain boundaries (Figure 6c). To be more specific, the polyhedron (octahedron deformation: i.e., A and B) shape indicates a crystallization through a preferred growth direction (111) ensuring a lower surface energy. Meanwhile, the corresponding particles size distribution (Figure 6d) shows that the size slightly increases from 32 to 46 nm after the postannealing at 500°C , and greatly increases to 745 nm when the temperature is 700°C . In the literature reported by Xiao et al.,²⁴ a large sintering effect was observed for vanadium dioxide particles in the same temperature ranges. Indeed, a similar large increase of VO_2 particle size is correlated to the huge endothermic peak at 675°C from DSC data. Those authors also discussed that the aggregation effect decreased drastically because of the low particles surface energy, and well-isolated VO_2 particles were observed, especially when the particle size was larger than 500

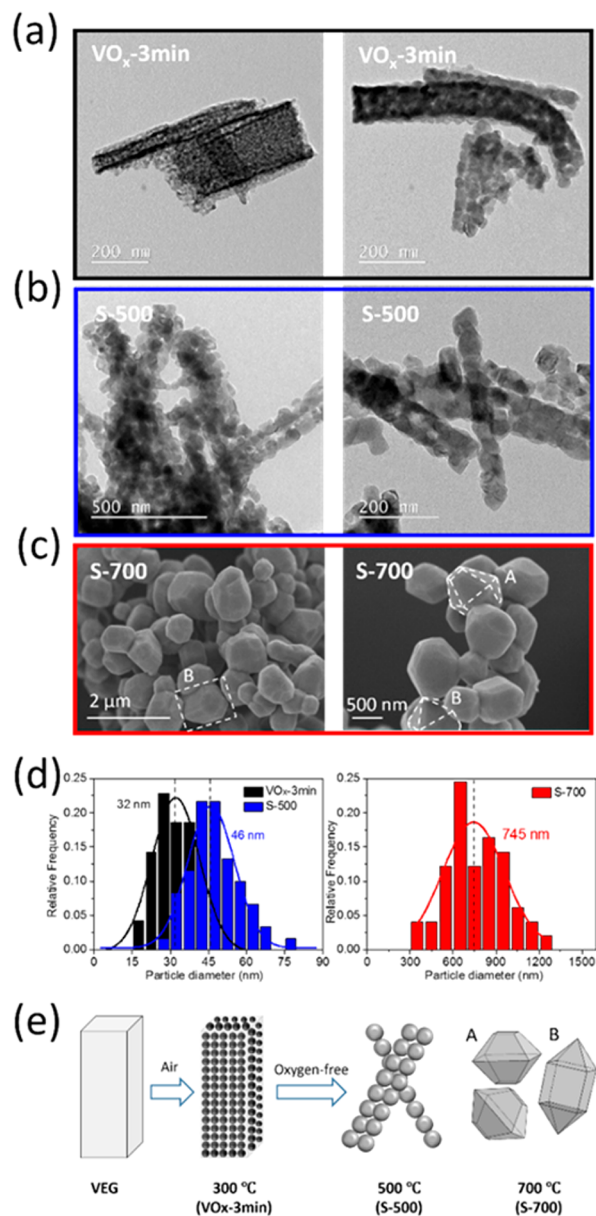


Figure 6. TEM and SEM images of the as-prepared VO_2 (M) particles synthesized with conditions (a) VO_x -3 min: 300°C for 3 min in air through decomposition of VEG; (b) S-500: post annealing treatment of VO_x -3 min at 500°C for 5 h in oxygen-free atmosphere; (c) S-700: post annealing of VO_x -3 min at 700°C for 5 h in oxygen-free atmosphere. (d) Size distribution of the as-prepared VO_2 particles. (e) Schematic illustration of the morphological evolution for VO_2 particles. (A and B designate two kinds of deformed octahedra).

Table 1. Lattice Parameters and Atomic Positions of VO_2 (M) (S-700)

| | | | | |
|-----------------|-------------------------------|-------------|-------------|--------------|
| space group | $P1\ 21/c\ 1$ (14) monoclinic | | | |
| cell parameters | a | b | c | β |
| | 5.7550(1) Å | 4.5291(7) Å | 5.3854(8) Å | 122.6030(4)° |
| atom | Wyck position | x | y | z |
| V1 | 4e | 0.2393(6) | 0.408(2) | 0.0266(6) |
| O1 | 4e | 0.095(2) | 0.216(2) | 0.198(2) |
| O2 | 4e | 0.408(2) | 0.720(2) | 0.308(2) |

nm. The evolution of the morphology from VEG to S-700, is schematized in Figure 6e.

To determine the nature and the proportion of the various components present in the three kinds of VO₂ powders, powder X-ray diffraction was used (Figure 7). The quantification analysis, using Rietveld refinement with the Fullprof program,²⁵ was deduced from the scale factor of the different phases either amorphous or crystalline.²⁶

An amount of calibration salt: lanthanum hexaboride (LaB₆), mixed as 10 wt % with the three VO₂ samples (VO_x-3 min, S-500 and S-700), is used as reference for calculation of the components proportions. The Rietveld refinement results are displayed in Figure 7a–c, showing a good-quality fit. The diffraction peaks at $2\theta = 27.95^\circ$ (Figure 7d), corresponding to the preferred (011) orientation of VO₂ (M), are thinner and of higher intensity for the annealed VO₂ powders (S-500 and S-700). The decrease of full width at half-maximum (fwhm) from 0.554° to 0.292° and 0.162° after the postannealing treatment at 500 and 700 °C, confirms the trend of the increase in average crystallite size in agreement with the TEM and SEM results in Figure 6. In addition to the larger crystallite sizes after being postannealed, the crystallinity of VO₂ particles also increases significantly. Deduced from the XRD patterns and analysis with the Fullprof program (Figure 7a–c), the weight percent of each component (including amorphous VO₂) in VO₂ powders is plotted in Figure 7e. The weight percent of crystalline VO₂ increases from 44% to 79% after postannealing at 500 °C (S-500). Furthermore, it reaches 100% for a postannealing temperature 700 °C (S-700). The proportion of crystallized VO₂ is improved clearly after postannealing in oxygen-free atmosphere. The enhanced crystallinity of VO₂ (M) should promote its thermochromic effect and make it more stable in the air environment.

It is well-known that the first order phase transition of VO₂ (M) occurs at around 68 °C with a large variation of latent heat. The DSC analysis of the three synthesized VO₂ samples (VO_x-3 min, S-500 and S-700) was measured using the same conditions (heating rate: 5 °C/min, atmosphere: Ar, and in between –30 and 110 °C) for both heating and cooling cycles (Figure 8). The endothermic and exothermic peaks during heating and cooling cycles are clearly visible. After postannealing, a more obvious phase transition of S-500 and S-700 samples compared with the initial VO₂ (M) powder (VO_x-3 min sample) is observed. To be more specific, the phase change enthalpy (ΔH) during the heating cycle increases greatly from 3.824 J/g to 40.837 J/g and 43.656 J/g, which is considerably high, and similar to the highest latent 43 J/g of the fine crystalline VO₂ nanoparticles reported by Chen et al.²⁷ and close to 51 J/g of bulk VO₂. The high latent could be attributed to the increase of crystalline VO₂ percentage in the powder. As for the two or three convoluted exothermic peaks detected in the cooling period, they probably result from a series of effects combination, including defects, lattice expansion, size effects, and nonstoichiometry of synthesized VO₂ powders.²⁷

3.2.2. Synthesis of V₂O₅ and V₂O₃. In addition to the synthesis of VO₂ (M), this two-step thermolysis and annealing method is also suitable for the preparation of V₂O₃ and V₂O₅ using VO_x-3 min as the starting material annealed under different conditions. The formation temperature of V₂O₃ and V₂O₅ is deduced from the thermogravimetric curve of VO_x-3 min in Figure 9a, revealing that the sample mass is stable when VO_x-3 min is annealed up to 800 °C in Ar flow with 5% H₂ or

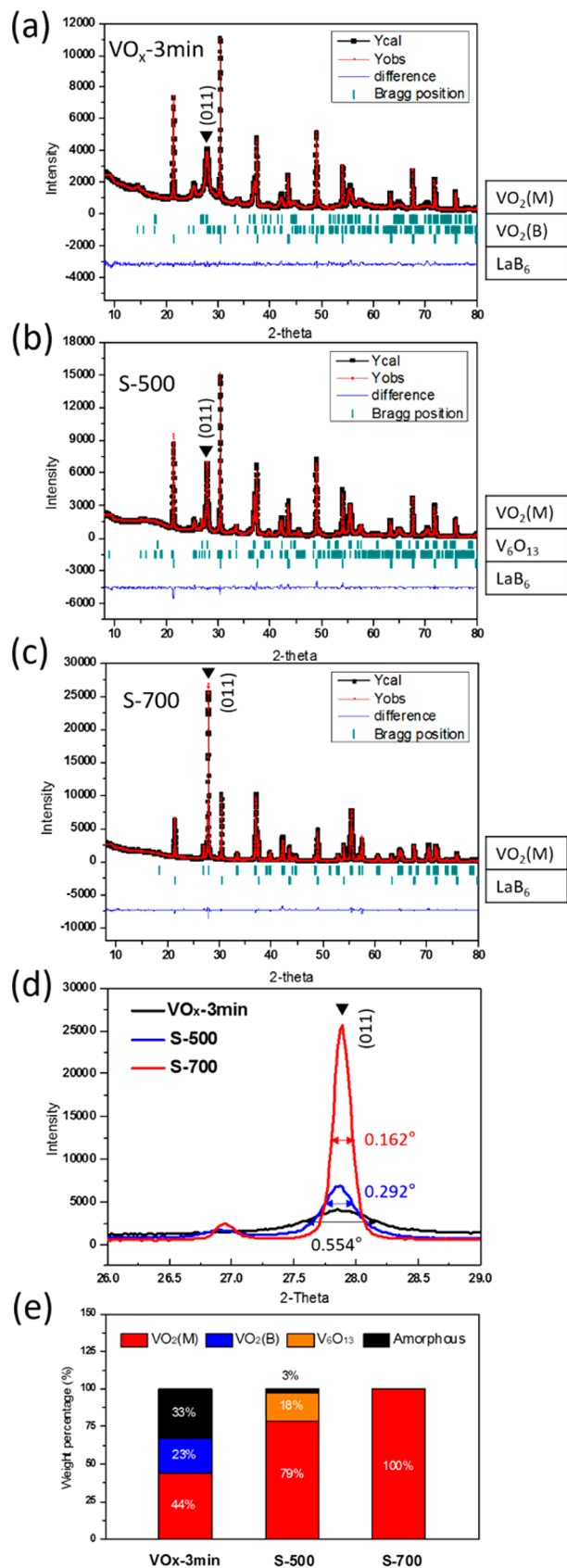


Figure 7. Typical Rietveld refinements of XRD data from (a) VO_x-3 min; (b) S-500; (c) S-700; (d) comparison of XRD peak at $2\theta = 27.95^\circ$ preferred (011) orientation for VO₂ (M); (e) and the corresponding weight percentage of each component.

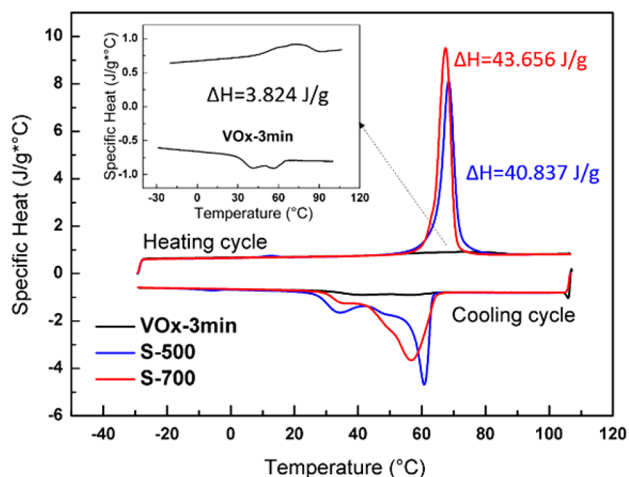


Figure 8. DSC curves of VO₂ samples of VO_x-3 min (inset shows its enlargement of DSC data), S-500, and S-700.

up to 600 °C in air. XRD shows that V₂O₃ and V₂O₅ are well obtained after annealing (Figure 9b). Interestingly, SEM results (Figure 9c) reveal that the V₂O₃ powder shows an urchin-like morphology with a high specific surface area, which can be of great interest for the use of vanadium sesquioxide as battery materials; i.e., such morphology is able to provide a large number of active sites between the active materials and electrolytes.^{28,29} Moreover, the morphology of as-prepared V₂O₅ exhibits regular plates, which can be of great advantage in terms of the lithium storage property for the use as positive electrode in batteries or electrochemical layer.³⁰ Their morphological evolution is schematized in Figure 9d. Thanks to this new synthesis protocol, we are able to produce different morphologies, as V₂O₃ and V₂O₅ synthesized with this two-step thermolysis and annealing differ from the ones obtained by direct annealing of VEG as earlier reported.²¹ Further investigations on their physical and chemical properties are under progress.

4. CONCLUSION

Herein, the decomposition of vanadyl ethylene glycolate (VEG), leading to VO₂ (M) particles with tunable crystallinity and morphology, through a two-step thermal treatment, a first-thermolysis step under air followed by postannealing under an oxygen-free atmosphere, has been investigated. Careful control of the time and the temperature parameters for the VEG thermolysis (first step) is required to obtain a pure VO₂ phase after the postannealing (second step). The use of shorter or longer time than ~3 min of heating at 300 °C for VEG decomposition results, after the postannealing, in the formation V(III) or V(V) compounds, respectively. While the thermolysis step is performed with a strict time of 3 min at 300 °C, a pure VO₂ (M) compound is synthesized with various crystallite sizes depending on the temperature of the postannealing treatment under an oxygen-free atmosphere (500 or 700 °C). SEM and TEM observations show an increase in the crystallite sizes of the VO₂ (M) powders with temperature up to few microns for 700 °C postannealing temperature, while the crystallite shapes become regular polyhedra. Moreover, thanks to XRD analyses (Rietveld refinements), the weight percent of the crystalline VO₂ (M) phase in the powders obtained after the 300 °C thermolysis, after 500 °C postannealing, or after 700 °C postannealing is

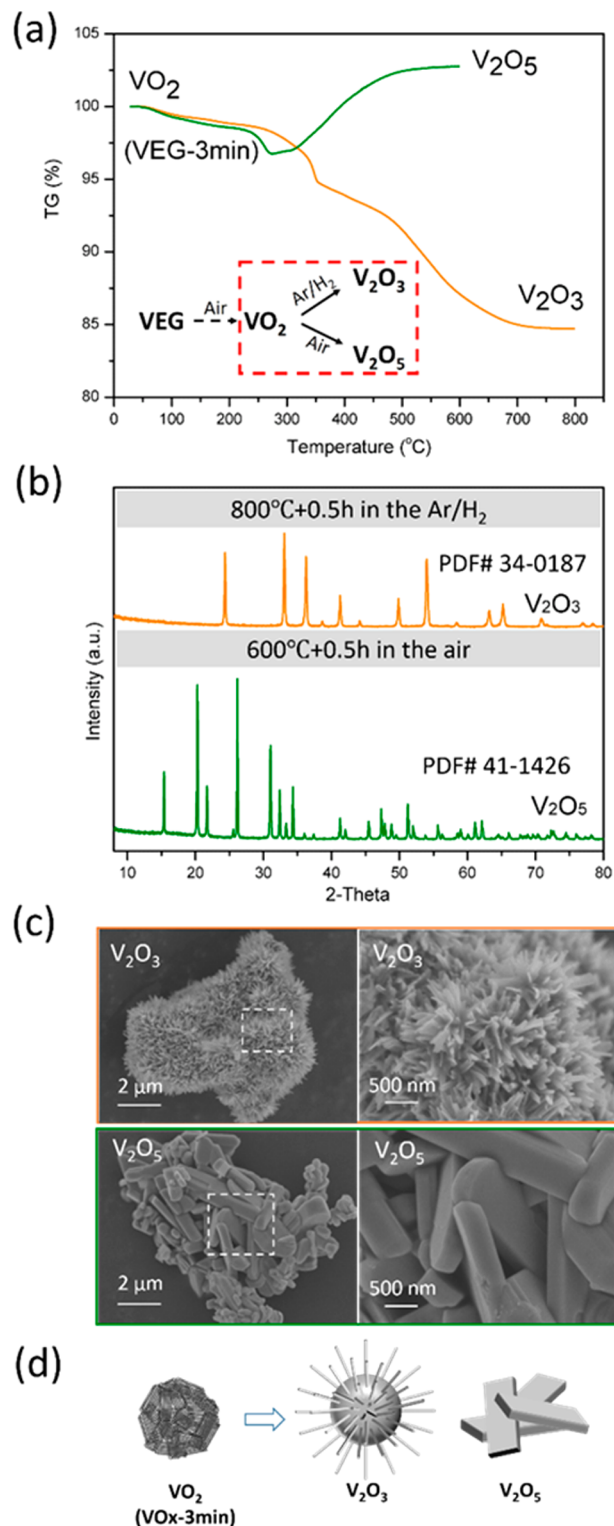


Figure 9. (a) TG curves of VO_x-3 min samples annealing under Ar/H₂ flow and air atmosphere; insets show the synthesis route of V₂O₃ and V₂O₅ from VO_x-3 min; (b) XRD pattern of V₂O₃ and V₂O₅ samples after postannealing of VO_x-3 min, (c) its corresponding SEM images, and (d) schematic illustration of the morphological evolution.

calculated. It increases from 44% to 79% reaching finally 100%. Hence, our synthesis protocol, a low cost and easy to implement synthesis route, allows us to obtain a pure and 100% crystalline VO₂ (M) phase using optimal conditions.

Additionally, V_2O_3 and V_2O_5 oxides with particular morphologies were synthesized from a similar two-step process by only modifying the atmosphere of the postannealing treatment, namely, reductive H_2 -Ar atmosphere for the former with a lower V(III) oxidation state and air atmosphere for the latter with a higher V(V) oxidation state.

■ ASSOCIATED CONTENT

● Supporting Information

The Supporting Information is available free of charge on the ACS Publications website at DOI: [10.1021/acs.inorgchem.8b00753](https://doi.org/10.1021/acs.inorgchem.8b00753).

Page S1, Table S1: CHNS analysis results on VO_2 compounds versus their thermal history. Page S2, Figure S1: Morphological analyses of the V_2O_3 sample: SEM, TEM, and HRTEM investigations (PDF)

■ AUTHOR INFORMATION

Corresponding Author

*E-mail: manuel.gaudon@icmcb.cnrs.fr.

ORCID

Aline Rougier: [0000-0002-1340-734X](https://orcid.org/0000-0002-1340-734X)

Manuel Gaudon: [0000-0002-6918-2004](https://orcid.org/0000-0002-6918-2004)

Funding

The Ph.D. grant of S.G. was supported by the China Scholarship Council.

Notes

The authors declare no competing financial interest.

■ ACKNOWLEDGMENTS

The authors would like to thank Eric Lebraud, Sonia Buffière, and Laetitia Etienne for their assistance during XRD, SEM & TEM, CHNS and DSC measurements, and Issam Mjejri for helpful discussion. All authors contributed to the discussions and revisions of the manuscript.

■ REFERENCES

- (1) Yu, W.; Li, S.; Huang, C. Phase evolution and crystal growth of VO_2 nanostructures under hydrothermal reactions. *RSC Adv.* **2016**, *6*, 7113.
- (2) Alie, L.; Gedvilas, D.; Wang, Z.; Tenent, R.; Engtrakul, C.; Yan, Y.; Shaheen, S. E.; Dillon, A. C.; Ban, C. Direct synthesis of the thermochromic VO_2 through hydrothermal reaction. *J. Solid State Chem.* **2014**, *212*, 237.
- (3) Mutta, G. R.; Popuri, S. R.; Vasundhara, M.; Maciejczyk, M.; Racu, A. V.; Banica, R.; Robertson, N.; Wilson, J. I. B.; Bennett, N. Facile hydrothermal synthesis of economically viable $VO_2(M1)$ counter electrode for dye sensitized solar cells. *S. Mater. Res. Bull.* **2016**, *83*, 135.
- (4) Batista, C.; Ribeiro, R. M.; Teixeira, V. Synthesis and characterization of VO_2 -based thermochromic thin films for energy-efficient windows. *Nanoscale Res. Lett.* **2011**, *6*, 301.
- (5) Cao, X.; Thet, M. N.; Zhang, Y.; Joachim Loo, S. C.; Magdassi, S.; Yan, Q.; Long, Y. Solution-based fabrication of VO_2 (M) nanoparticles via lyophilisation. *RSC Adv.* **2015**, *5*, 25669.
- (6) Cao, Z.; Xiao, X.; Lu, X.; Zhan, Y.; Cheng, H.; Xu, G. A simple and low-cost combustion method to prepare monoclinic VO_2 with superior thermochromic properties. *Sci. Rep.* **2016**, *6*, 39154.
- (7) Chen, X.; Wang, X.; Wang, Z.; Wan, J.; Liu, J.; Qian, Y. An ethylene glycol reduction approach to metastable VO_2 nanowire arrays. *Nanotechnology* **2004**, *15*, 1685.
- (8) Dahlman, C. J.; LeBlanc, G.; Bergerud, A.; Staller, C.; Adair, J.; Milliron, D. J. Electrochemically Induced Transformations of Vanadium Dioxide Nanocrystals. *Nano Lett.* **2016**, *16*, 6021.
- (9) Li, G.; Chao, K.; Peng, H.; Chen, K.; Zhang, Z. Low-Valent Vanadium Oxide Nanostructures with Controlled Crystal Structures and Morphologies. *Inorg. Chem.* **2007**, *46*, 5787.
- (10) Liu, J.; Li, Q.; Wang, T.; Yu, D.; Li, Y. Metastable Vanadium Dioxide Nanobelts: Hydrothermal Synthesis, Electrical Transport, and Magnetic Properties. *Angew. Chem.* **2004**, *116*, 5158.
- (11) Zhang, P.; Jiang, K.; Deng, Q.; You, Q.; Zhang, J.; Wu, J.; Hu, Z.; Chu, J. Manipulations from oxygen partial pressure on the higher energy electronic transition and dielectric function of VO_2 films during a metal-insulator transition process. *J. Mater. Chem. C* **2015**, *3*, 5033.
- (12) Chen, Z.; Gao, Y.; Kang, L.; Du, J.; Zhang, Z.; Luo, H.; Miao, H.; Tan, G. VO_2 -based double-layered films for smart windows: Optical design, all-solution preparation and improved properties. *Sol. Energy Mater. Sol. Cells* **2011**, *95*, 2677.
- (13) Gonçalves, A.; Resende, J.; Marques, A. C.; Pinto, J. V.; Nunes, D.; Marie, A.; Goncalves, R.; Pereira, L.; Martins, R.; Fortunato, E. Smart optically active VO_2 nanostructured layers applied in roof-type ceramic tiles for energy efficiency. *Sol. Energy Mater. Sol. Cells* **2016**, *150*, 1.
- (14) Melnik, V.; Khatsevych, I.; Kladko, V.; Kuchuk, A.; Nikirin, V.; Romanyuk, B. Low-temperature method for thermochromic high ordered VO_2 phase formation. *Mater. Lett.* **2012**, *68*, 215.
- (15) Zhou, J.; Gao, Y.; Zhang, Z.; Luo, H.; Cao, C.; Chen, Z.; Dai, L.; Liu, X. VO_2 thermochromic smart window for energy savings and generation. *Sci. Rep.* **2013**, *3*, 3029.
- (16) Nag, J.; Haglund, R. F., Jr. Synthesis of vanadium dioxide thin films and nanoparticles. *J. Phys.: Condens. Matter* **2008**, *20*, 264016.
- (17) Wang, N.; Magdassi, S.; Mandler, D.; Long, Y. sol-gel process and one-step annealing of vanadium dioxide thin films: Synthesis and thermochromic properties. *Thin Solid Films* **2013**, *534*, 594.
- (18) Hou, J.; Wang, Z.; Ding, Z.; Zhang, Z.; Zhang, J. Facile synthesize VO_2 (M1) nanorods for a low-cost infrared photodetector Application. *Sol. Energy Mater. Sol. Cells* **2018**, *176*, 142.
- (19) Zheng, C.; Zhang, X.; Zhang, J.; Liao, K. Preparation and Characterization of VO_2 Nanopowders. *J. Solid State Chem.* **2001**, *156*, 274.
- (20) Choi, Y.; Sim, D. M.; Hur, Y. H.; Han, H. J.; Jung, Y. S. Synthesis of colloidal VO_2 nanoparticles for thermochromic applications. *Sol. Energy Mater. Sol. Cells* **2018**, *176*, 266.
- (21) Mjejri, I.; Rougier, A.; Gaudon, M. Low-Cost and Facile Synthesis of the Vanadium Oxides V_2O_3 , VO_2 , and V_2O_5 and Their Magnetic, Thermochromic and Electrochromic Properties. *Inorg. Chem.* **2017**, *56*, 1734.
- (22) Zhang, H.; Xiao, X.; Lu, X.; Chai, G.; Sun, Y.; Zhan, Y.; Xu, G. A cost-effective method to fabricate VO_2 (M) nanoparticles and films with excellent thermochromic properties. *J. Alloys Compd.* **2015**, *636*, 106.
- (23) Zou, J.; Peng, Y.; Lin, H. A low-temperature synthesis of monoclinic VO_2 in an atmosphere of air. *J. Mater. Chem. A* **2013**, *1*, 4250.
- (24) Xiao, X.; Zhang, H.; Chai, G.; Sun, Y.; Yang, T.; Cheng, H.; Chen, L.; Miao, L.; Xu, G. A cost-effective process to prepare VO_2 (M) powder and films with superior thermochromic properties. *Mater. Res. Bull.* **2014**, *51*, 6.
- (25) Pawar, R. A.; Patange, S. M.; Shirsath, S. E. Spin glass behavior and enhanced but frustrated magnetization in Ho^{3+} substituted Co-Zn ferrite interacting nanoparticles. *RSC Adv.* **2016**, *6*, 76590.
- (26) Masudi, M.; Hashim, M.; Kamari, H. M.; Salit, M. S. A General Method for Quantifying the Amorphous Phase in Nano Polycrystalline Materials. *Mod. Appl. Sci.* **2012**, *6*. DOI: [10.5539/mas.v6n6p1](https://doi.org/10.5539/mas.v6n6p1)
- (27) Chen, Z.; Gao, Y.; Kang, L.; Cao, C.; Chen, S.; Luo, H. J. Fine crystalline VO_2 nanoparticles: synthesis, abnormal phase transition temperatures and excellent optical properties of a derived VO_2 nanocomposite foil. *J. Mater. Chem. A* **2014**, *2*, 2718.

(28) Liu, H.; Wang, Y.; Li, H.; Yang, W.; Zhou, H. Flowerlike Vanadium Sesquioxide: Solvothermal Preparation and Electrochemical Properties. *ChemPhysChem* **2010**, *11*, 3273.

(29) Xu, Y.; Zheng, L.; Wu, C.; Qi, F.; Xie, Y. New-Phased Metastable V_2O_3 Porous Urchinlike Micronanostructures: Facile Synthesis and Application in Aqueous Lithium Ion Batteries. *Chem. - Eur. J.* **2011**, *17*, 384.

(30) Zhang, C.; Fang, G.; Liang, C.; Zhou, J.; Tan, X.; Pan, A.; Liang, S. Template-free synthesis of highly porous V_2O_3 cuboids with enhanced performance for lithium ion batteries. *Nanotechnology* **2016**, *27*, 305404.

(31) Akande, A. A.; Liganiso, E. C.; Dhonge, B. P.; Rammutla, K. E.; Machatine, A.; Prinsloo, L.; Kunert, H.; Mwakikunga, B. W. Phase evolution of vanadium oxides obtained through temperature programmed calcinations of ammonium vanadate in hydrogen atmosphere and their humidity sensing properties. *Mater. Chem. Phys.* **2015**, *151*, 206–214.